HIGH-RESOLUTION GAMMA-RAY SPECTROSCOPY WITH ELIADE AT THE EXTREME LIGHT INFRASTRUCTURE*

P.-A. Söderström[a], G. Suliman[a], C.A. Ur[a], D. Balabanski[a]
T. Beck[b], L. Capponi[a], A. Dhal[a], V. Iancu[a], S. Ilie[a], M. Iovea[c]
A. Kuşoğlu[a,d], C. Petcu[a], N. Pietralla[b], G.V. Turturică[a]
E. Udup[a], J. Wilhelmy[e], A. Zilges[e]

[a]Extreme Light Infrastructure–Nuclear Physics (ELI–NP)
077125 Bucharest-Măgurele, Romania
[b]Institut für Kernphysik, TU Darmstadt, 64289 Darmstadt, Germany
[c]ACCENT PRO 2000, S.R.L.
Nerva Traian 1, K6, Apt. 26, 031041 Bucharest, Romania
[d]Department of Physics, Faculty of Science, Istanbul University
Vezneciler/Fatih, 34134 Istanbul, Turkey
[e]Institut für Kernphysik, University of Cologne, 50937 Köln, Germany

(Received November 21, 2018)

The Extreme Light Infrastructure is a major European undertaking with the aim of constructing a set of facilities that can produce the worlds highest intensity laser beams as well as unique high-brilliance, narrow-bandwidth gamma-ray beams using laser-based inverse Compton scattering. The latter will be one of the unique features of the facility in Bucharest-Măgurele, Romania, where the scientific focus will be towards nuclear physics and nuclear photonics both with high intensity lasers and gamma beams individually, as well as combined. One of the main instruments being constructed for the nuclear physics and applications with high-brilliance gamma-beams research activity is the ELIADE γ-ray detector array. This array consists of eight segmented HPGe clover detectors as well as large-volume $LaBr_3$ detectors. The nuclear physics topics are expected to cover a large range including, but not limited to, properties of pygmy resonance and collective scissors mode excitations, parity violation in nuclear excitations, and matrix elements for neutrinoless double-beta decay. However, the uniqueness of the environment in which ELIADE will operate presents several challenges in the design and construction of the array. Here, we discuss some of these challenges and how we plan to overcome them, as well as the current status of implementation.

DOI:10.5506/APhysPolB.50.329

* Presented at the Zakopane Conference on Nuclear Physics "Extremes of the Nuclear Landscape", Zakopane, Poland, August 26–September 2, 2018.

1. Introduction

With the invention of chirped pulse amplification for lasers [1], the path towards high-power laser systems all over the world has been paved. One of these, in particular, is the Extreme Light Infrastructure (ELI), a new Research Infrastructure of pan-European interest and part of the European Strategy Forum on Research Infrastructures (ESFRI) Roadmap. ELI will become the most intense laser beam-line system worldwide divided into four pillars three of which are: ELI Beamlines, Dolní Břežany, Prague, Czech Republic; ELI Attosecond Light Pulse Source, Szeged, Hungary; and ELI Nuclear Physics (ELI–NP), Măgurele, Romania. The location of the fourth pillar, the high-intensity pillar with projected laser intensity up to 100 PW, is still to be decided.

One of the unique features of ELI–NP is that there will be, in addition to the high-power laser system [2], also an additional high-brilliance gamma beam system (GBS) [3]. This adds two additional layers of possible physics topics to be explored. One of these layers is the interaction of the high-power laser with the gamma beam including topics such as the production of isomers in stellar conditions, study of non-perturbative treatments, pair production and $\gamma\gamma$ scattering within quantum electrodynamics, and vacuum birefringence to name a few [4]. The second aspect is the stand-alone use of the GBS for photonuclear reaction studies and is the topic that will be discussed further in these proceedings.

2. Physics with the gamma-beam system

The GBS proposed [3] for ELI–NP is projected to outperform existing facilities with an order of magnitude both with respect to intensity as well as bandwidth. For example, the NewSUBARU facility [5] in Japan has a γ-ray intensity of $\sim 10^5$ γ/s with a bandwidth of down to 1% [6]. In the US, the HIγS facility [7] is the leading facility for nuclear physics with a γ-ray intensity of $\sim 10^7$ γ/s with a bandwidth of 1–10% [6]. Within the framework of the technical design report [3], at ELI–NP the beam will be produced via Compton backscattering of laser pulses from a 100 Hz of Yb:YAG laser off up to 720 MeV electrons delivered by a warm LINAC. This will provide γ rays in the energy range between 200 keV and 19.5 MeV, with a bandwidth of $\leq 0.5\%$ and an intensity exceeding 5×10^8 γ/s [6]. Furthermore, a linear beam polarization of up to 100% will be possible at ELI–NP.

Several different experimental setups are under construction at ELI–NP for various topics within nuclear physics experiments. These include Nuclear Resonance Fluorescence (NRF) spectroscopy using (γ, γ') reactions [8] and neutron emission from pygmy- and giant resonances using (γ, n) reactions [9]. Using charged particle detectors for heavy ions and light particles

photo-induced fission [10] and properties of key astrophysics (γ, p) and (γ, α) reactions [11] will be studied. In addition, the GBS will be used for both for industry, non-proliferation, and cultural heritage applications [12], and to produce a high-intensity positron beam-line for material research [13].

2.1. Nuclear Resonance Fluorescence

The basic principle of the Nuclear Resonance Fluorescence (NRF) technique is the resonant absorption of a photon of an excited state in a nucleus, with a probability proportional to the partial ground-state decay width, Γ_0, and the subsequent decay either into the ground state or into intermediate energy levels, usually called resonant γ-ray scattering. These scattered photons, detected by a γ-ray spectrometer, carry information regarding the total level width, Γ, as well as the branchings, Γ_i/Γ to excited state i. As these widths are related to the life times of the states, their measured values can, furthermore, be used as an independent tool to compare reduced transition probabilities obtained from other methods such as Coulomb excitation or various direct life-time measurements.

The NRF method is particularity attractive as it provides a very selective excitation, compared to, for example, excitation based on the Coulomb field of an incoming heavy ion. Furthermore, with the ability to not only control the energy of the incoming beam precisely, the ability to control the polarization of the beam gives precise and model-independent access to other key nuclear physics observables such as parity of the states and multipolarity mixture of the decays. For an in-depth review of the NRF concept, see Ref. [14].

3. The ELIADE HPGe γ-ray spectrometer

Within the framework of ELI–NP, in particular for experiments with the GBS, a setup was proposed to perform NRF measurements taking advantage of the unique features of the GBS. The detectors chosen for this purpose, ELIADE (ELI Array of DEtectors), consist of eight similar segmented HPGe Clover detectors where each crystal is divided into eight segments in a similar manner to the TIGRESS [15] array at TRIUMF in Canada. ELIADE can be used both in the low-energy experimental area E2 and the high-energy experimental area E8. For an illustration of the latter see Fig. 1. The geometry of ELIADE was chosen in such a way that it has a central ring at 90° with two detectors horizontal and two detectors vertical to the beam axis to maximize the sensitivity to E1 and M1 transitions. In addition, a second ring of four detectors at 135° is included to increase the sensitivity to E2 transitions.

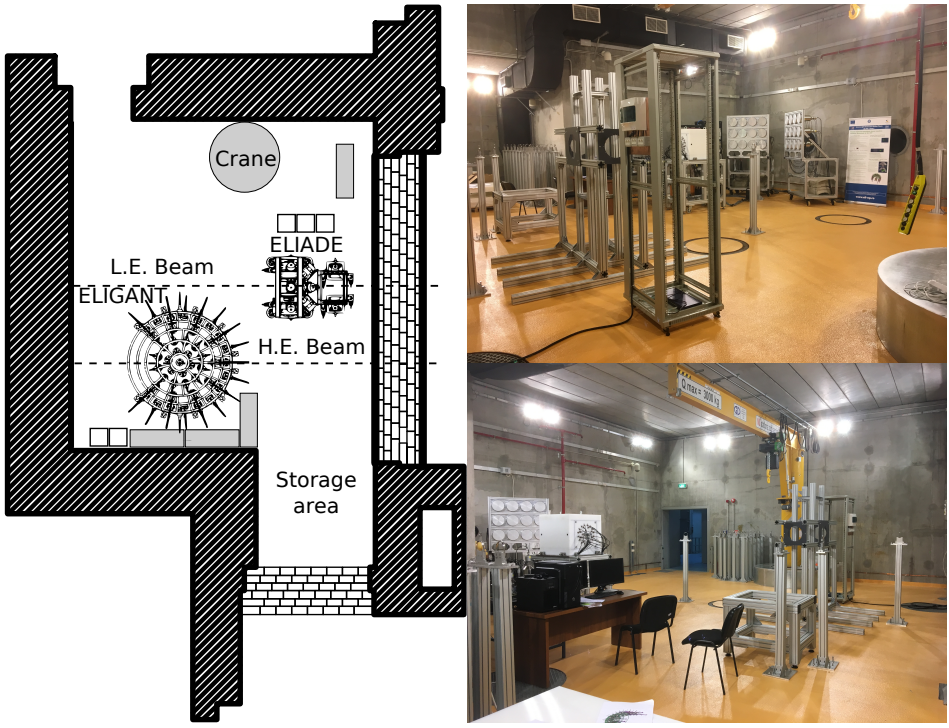

Fig. 1. Illustration of the high-energy experimental area E8 with possible location of electronics (white boxes) and tables (gray boxes). In this illustration, ELIADE is in the low-energy (L.E.) beam-line and ELIGANT in the high-energy (H.E.) beam-line. Photos are the installation status as of 2018-08-08.

One challenge for spectroscopy with the GBS at the environment in ELI–NP is the high intensity of the beam that will produce a very large γ-ray background. Furthermore, this background will be strongly correlated with the time structure of the beam that consists of a macro-pulse repetition rate of 100 Hz with a train of 32 micro-pulses separated by 16 ns within each macro-pulse. This background comes both from pair-production of electrons and positrons that result in a strong 511 keV background γ-ray as well as Compton scattering of the beam itself directly into the ELIADE detectors. To resolve this, two methods will be used. Since a majority of the background consist of low-energy γ-rays, the first method is to shield the detectors with thick lead and/or copper attenuators. This will drastically reduce the efficiency for low-energy γ-rays while keeping acceptable efficiency for high-energy γ-rays. The second method is the use of segmented Clovers. In this way it is possible to reduce the counting rate to one γ ray per macro-pulse per segment and disentangle pile-up events based on energy deposition

in the individual segments compared to the full crystal, the known time-structure of the beam, and pulse-shape analysis by saving the first part of the digitized voltage pulses from the detector to disk.

To read out the detectors, a digital data acquisition system based on the CAEN v1725 14 bit and 250 MS/s digitizers will be used and read out using the MIDAS data acquisition framework. The signals will be transported from the detectors to the digitizers based on a dedicated system developed by the Institut für Kernphysik at the University of Cologne. In this case, the single-ended signals from the detector will be converted to much more noise resilient differential signals using electronics mounted on the ELIADE cryostats. The differential signals are transported using MDR cables to the electronics area, where another converter recreates the original single-ended signal. The high voltage for ELIADE will be provided by a CAEN SY4527 high-voltage module and the liquid nitrogen filling system will be controlled by a dedicated LabVIEW program running on a National Instruments compact RIO computer. An illustration of the system is shown in Fig. 2.

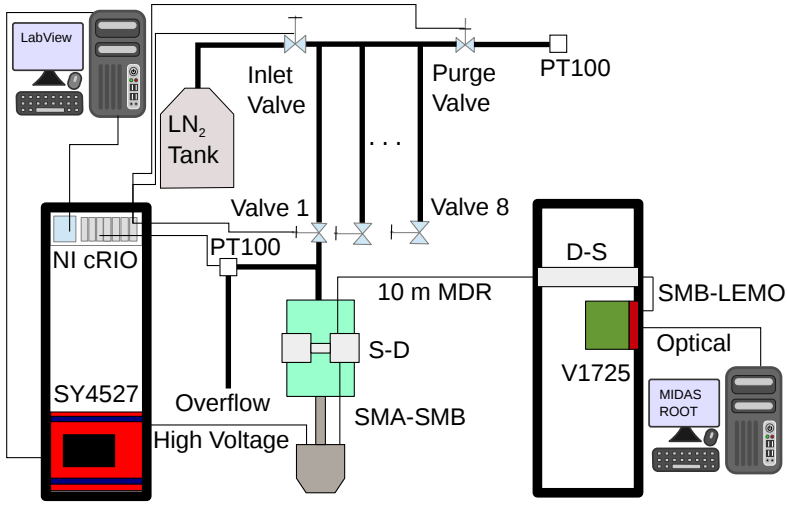

Fig. 2. Schematic coupling of ELIADE to parts of the hardware infrastructure. This includes the CAEN SY4527 high-voltage supply, the v1725 digitizer and the single–differential–single (S–D–S) transmission system, and the National Instruments compact RIO computer and the PT100 temperature sensors for liquid nitrogen cooling.

4. Day one physics cases and applications with ELIADE

Given the particular properties of the GBS, including the intensity, bandwidth, polarization and size of the beam spot, a few different physics con-

cepts have been highlighted in the technical design report [8]. These include the properties of the pygmy dipole resonance and the scissors mode, parity violation of the nuclear force, test of nuclear structure models for the neutrino-less double-β decay, magnetic dipole moments of actinides, and similar. Here, a few examples will be discussed in more detail.

4.1. Matrix elements for $0\nu\beta\beta$-decay

One of the experimental programs for the NRF setup relates to the nuclear structure input of experimental and theoretical work on neutrinoless double β-decay ($0\nu\beta\beta$), shown in Fig. 3. In particular, the rate of this type of decay, $\lambda_{0\nu\beta\beta}$, depends mainly on two variables: the neutrino mass, $\frac{\langle m_\nu \rangle}{m_e}$, and the nuclear matrix element, $\left|M^{(0\nu)}\right|$, as

$$\lambda_{0\nu\beta\beta} = G_{0\nu} \left|M^{(0\nu)}\right|^2 \left(\frac{\langle m_\nu \rangle}{m_e}\right)^2 . \tag{1}$$

Here, $G_{0\nu}$ is a kinematic factor. These matrix elements have to be calculated and depend strongly on the nuclear structure of the nuclei involved, in particular on the proton–neutron coupling. From a nuclear structure perspective, one way to constrain the proton–neutron coupling is through the

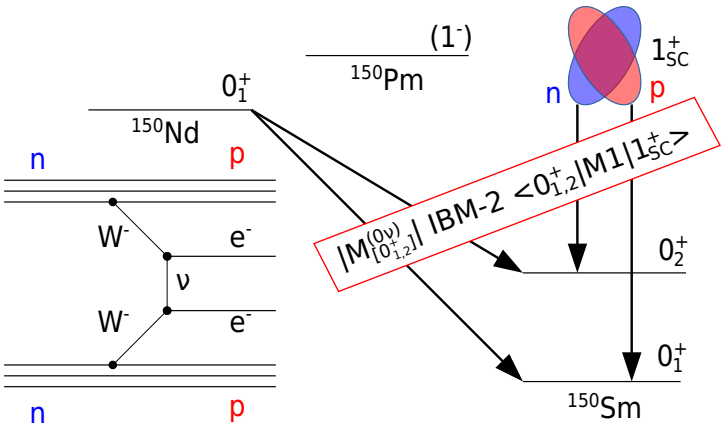

Fig. 3. Illustration of the $0\nu\beta\beta$-decay process where two neutrons (n) decaying into two protons (p) by simultaneously radiating a W^- boson which via the exchange of a virtual Majorana neutrono (ν) pair decays into two β-electrons (e^-). The process is illustrated through the $0\nu\beta\beta$ decay of ^{150}Nd into ^{150}Sm. Furthermore, the decay of the scissors mode state (1^+_{SC}) into the first to 0^+ states and how these matrix elements ($\langle 0^+_{1,2}|\mathrm{M1}|1^+_{SC}\rangle$) relates to the $0\nu\beta\beta$matrix element ($M^{(0\nu)}_{[0^+_{1,2}]}$) through the interacting boson model with proton–neutron degrees of freedom (IBM-2) is shown.

properties of the nuclear scissors mode. This is a nuclear excitation where the neutron and proton distribution in a deformed nucleus rotates out of phase from each other and, thus, the properties of these excitations are very sensitive to the proton-neutron coupling. In a recent publication, using bremsstrahlung radiation from the S-DALINAC electron linear accelerator in Darmstadt, Germany, ^{154}Gd was examined as a possible candidate and an unexpectedly large branching from the scissors mode to the 0_2^+ state was observed [16]. In the same reference, the decay from ^{150}Nd to ^{150}Sm was suggested to have an even larger contribution to 0_2^+. Thus, determining the parities of $J = 1$ states in the scissors mode region and measuring scissors branching to 0_2^+ will be one of the high-profile experiments at the operations start of the ELI–NP GBS.

4.2. Parity violation in ^{20}Ne

Another high-profile physics topic to be explored, illustrated in Fig. 4, is the conservation, or violation, of one of the fundamental symmetries in nature, parity. This symmetry is known to be fundamental in two of the four forces of the standard model; the electromagnetic and strong interactions. It is, however, shown to be violated in the weak interaction [17]. For nuclear physics, the effective nuclear force contains contributions from all three of the strongest forces and, thus, a small parity violating term, $\beta \sim 10^{-4}$, could appear in the construction of a negative parity state with spin J as

$$\left\langle J^- \right\rangle = \alpha \left\langle \phi^- \right\rangle + \beta \left\langle \phi^+ \right\rangle . \tag{2}$$

Here, the coefficient α contains most of the contribution from the wave functions $\phi^{\pm}$ separated into positive and negative parity components.

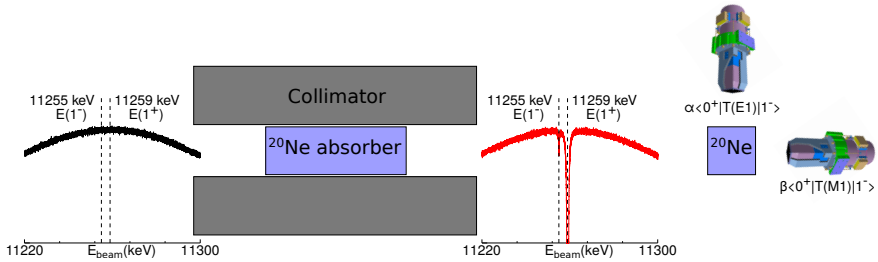

Fig. 4. Conceptual illustration for the measurement of the parity violating matrix elements in ^{20}Ne. The incoming beam (black) has a smooth energy distribution. After the thick absorber, the beam contain no γ rays in the resonant energy of the 11259 keV region. The two matrix elements are measured based on the difference yield in the vertical and horizontal plane of the ELIADE detector array.

One promising case to observe parity violation in practice is in the nucleus ^{20}Ne that has a $1^{\pm}$ parity doublet with a difference in energy of only $\Delta E = 3$–4 keV, located at approximately 11.2 MeV [18]. With an expected population of approximately a factor of 50 larger for the 1^{+} state and with the two states so close in energy, measurements of the parity mixing in the 1^{-} state are challenging. However, the large cross section also works in our favor as it makes it possible to filter out the 11.259 MeV γ rays using a thick absorber of ^{20}Ne within a collimator along the beam line. Even with a complete absorption of the 11.259 MeV γ rays, the 11.255 MeV γ rays should be sufficiently unaffected to selectively populate only the 1^{-} state. With a linear polarization of the beam of 100%, the mixing parameter β can then be measured from the angular distribution of the resonantly scattered γ rays as

$$\left\langle 0^{+}\right| T(E1)+T(M1)\left|1^{-}\right\rangle = \alpha\left\langle 0^{+}\right| T(E1)\left|\phi^{-}\right\rangle + \beta\left\langle 0^{+}\right| T(M1)\left|\phi^{+}\right\rangle \ . \quad (3)$$

Further details regarding the self-absorption experimental technique in combination with NRF can be found in Ref. [19].

4.3. NRF for applications

The concept of self-absorption for NRF can also be used for applications related to industry, cultural heritage and homeland security as the same resonant scattering process that are used to determine level widths also can be used to determine the quantity of the relevant isotope given the level widths of the scattering levels. One large difference compared to physics focused NRF is that the objects to be studied are often not of a size that is practical to be used in the center of an array. If the object is large, like a statuette or a container of nuclear fuel, one can instead use the self-absorption approach discussed for the case of ^{20}Ne. In this case, one or more isotopes of interest are selected and produced in a small enough size appropriate for an NRF scattering target. The object itself may be placed in front of a collimator and the beam will be attenuated when passing through the object, see Fig. 5. In particular, any nuclear resonances within the energy distribution of the beam will scatter the beam and produce absorption lines in the beam distribution before reaching the scattering foil. Comparing the ratio of NRF γ-rays scattered from the reference foils in ELIADE with the object and without it, the quantity of the relevant isotopes in the beam path can be estimated from the reduction of the γ-ray peaks in the HPGe spectra. In addition to ELIADE, such a measurement would also use a large volume detector for absolute normalization of the beam intensity due to Compton scattering within the object. This will provide a very clean image of the

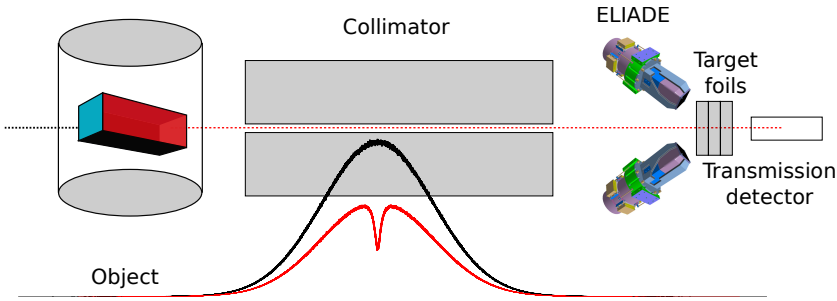

Fig. 5. (Colour on-line) Illustration of the use of the GBS with ELIADE for cultural heritage tomography. The unattenuated beam (black) and the attenuated beam (grey/red) imping on target foils containing the isotopes of interest and the image is reconstructed from the absorption lines in the data from the attenuated beam.

isotope content and together with a rotating and raisable table, one can prepare a detailed three-dimensional tomography of each isotope of interest in object under investigation [12].

5. Summary

We have given a brief introduction to the Extreme Light Infrastructure-Nuclear Physics facility currently under implementation. Our focus have been the possibilities of the gamma beam system, and the possibility to do γ-ray spectroscopy with high-purity germanium detectors. A few selected physics cases have been discussed in detail.

We would like to acknowledge the support from the Extreme Light Infrastructure–Nuclear Physics (ELI–NP) Phase II, a project co-financed by the Romanian Government and the European Union through the European Regional Development Fund — the Competitiveness Operational Programme (1/07.07.2016, COP, ID 1334). T.B., N.P., J.W., and A.Z. acknowledge the support from the German BMBF under grants No. 05P18RDEN9 and No. 05P2018PKEN9.

REFERENCES

[1] D. Strickland, G. Mourou, *Opt. Commun.* **56**, 219 (1985).
[2] D. Ursescu *et al.*, *Rom. Rep. Phys.* **68**, S11 (2016).
[3] H.R. Weller *et al.*, *Rom. Rep. Phys.* **68**, S447 (2016).
[4] K. Homma *et al.*, *Rom. Rep. Phys.* **68**, S233 (2016).

[5] H. Utsunomiya, S. Hashimoto, S. Miyamoto, *Nucl. Phys. News* **25**, 25 (2015).
[6] D. Filipescu *et al.*, *Eur. Phys. J. A* **51**, 185 (2015).
[7] H.R. Weller, M.W. Ahmed, Y.K. Wu, *Nucl. Phys. News* **25**, 19 (2015).
[8] C.A. Ur *et al.*, *Rom. Rep. Phys.* **68**, S483 (2016).
[9] F. Camera *et al.*, *Rom. Rep. Phys.* **68**, S539 (2016).
[10] D.L. Balabanski *et al.*, *Rom. Rep. Phys.* **68**, S621 (2016).
[11] O. Tesileanu *et al.*, *Rom. Rep. Phys.* **68**, S699 (2016).
[12] G. Suliman *et al.*, *Rom. Rep. Phys.* **68**, S799 (2016).
[13] N. Djourelov *et al.*, *Rom. Rep. Phys.* **68**, S735 (2016).
[14] U. Kneissl, N. Pietralla, A. Zilges, *J. Phys. G: Nucl. Part. Phys.* **32**, R217 (2006).
[15] H.C. Scraggs *et al.*, *Nucl. Instrum. Methods Phys. Res. A* **543**, 431 (2005).
[16] J. Beller *et al.*, *Phys. Rev. Lett.* **111**, 172501 (2013).
[17] C.S. Wu *et al.*, *Phys. Rev.* **105**, 1413 (1957).
[18] J. Beller *et al.*, *Phys. Lett. B* **741**, 128 (2015).
[19] D. Savran, J. Isaak, *Nucl. Instrum. Methods Phys. Res. A* **899**, 28 (2018).